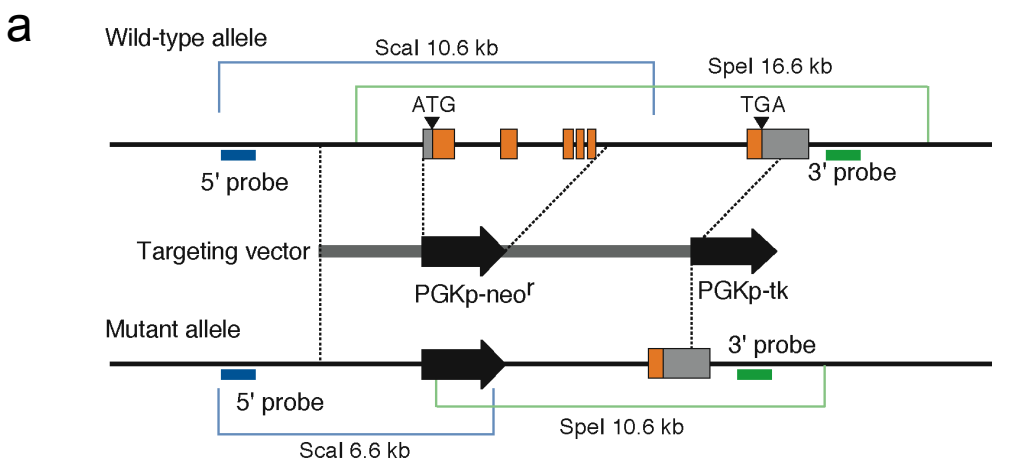

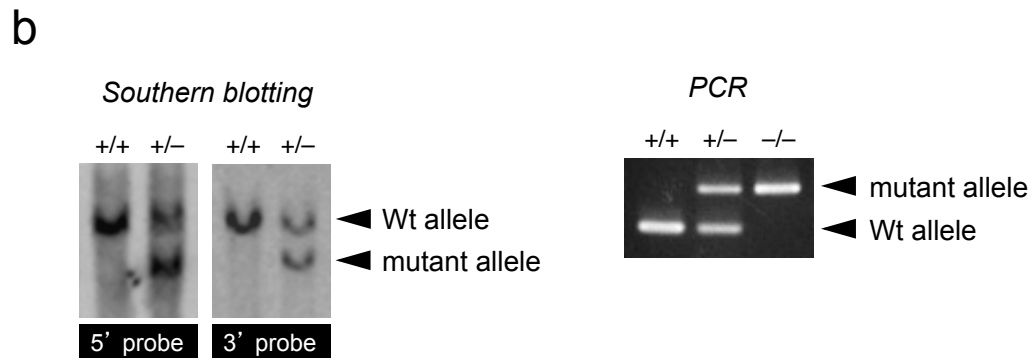

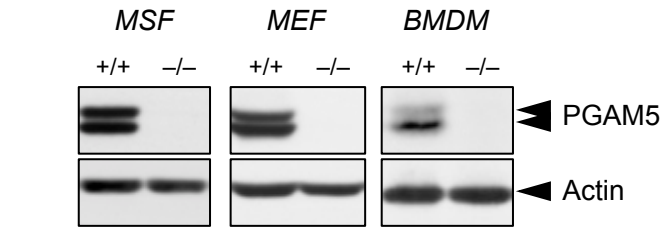

Supplementary Figure 1 Generation of Pgam5 knockout (KO) mice.

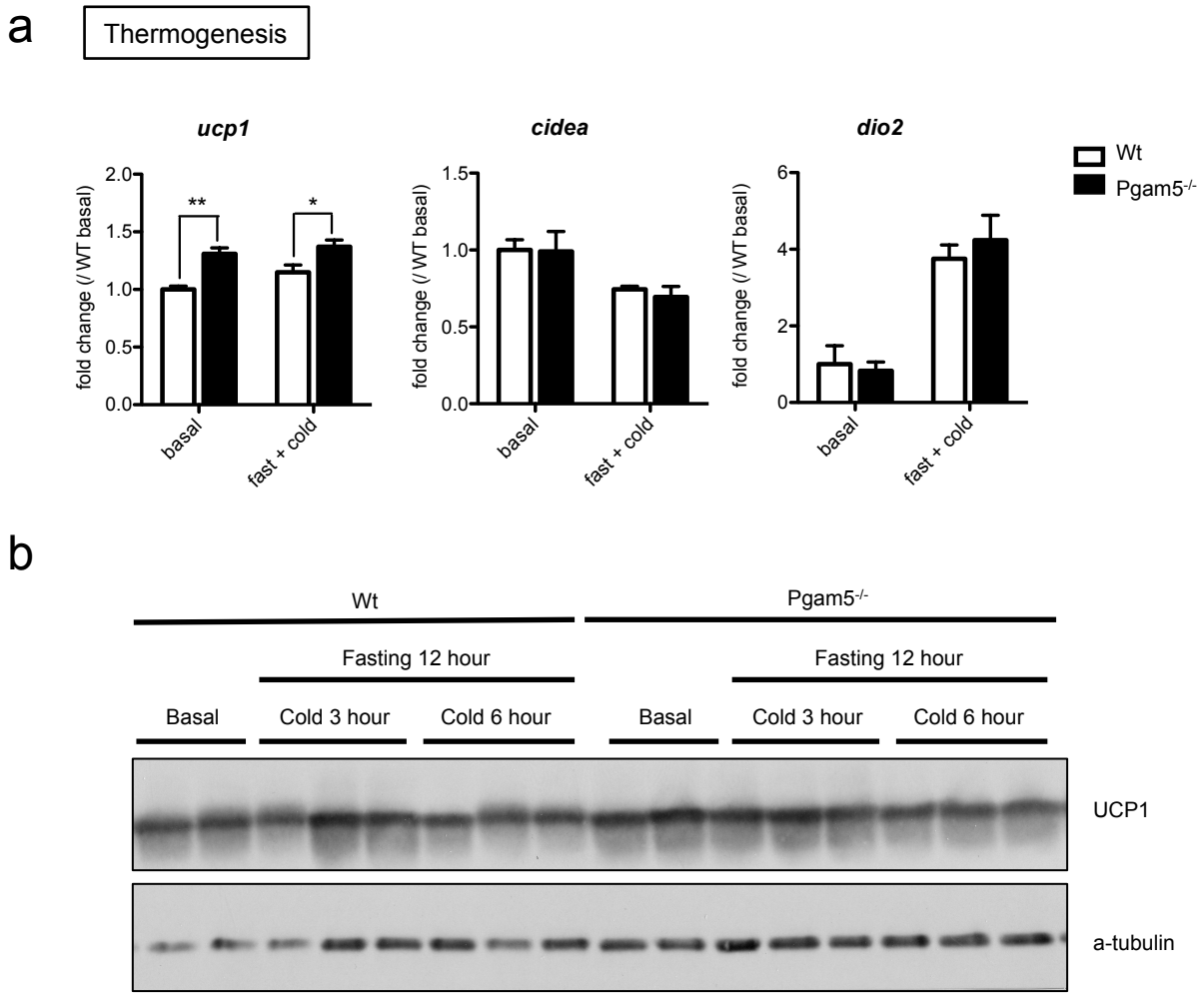

Supplementary Figure 2
The expression levels of several genes related to adaptive thermogenesis in Pgam5-KO-mice-derived brown adipose tissue (BAT) are comparable to those in Wt mice.

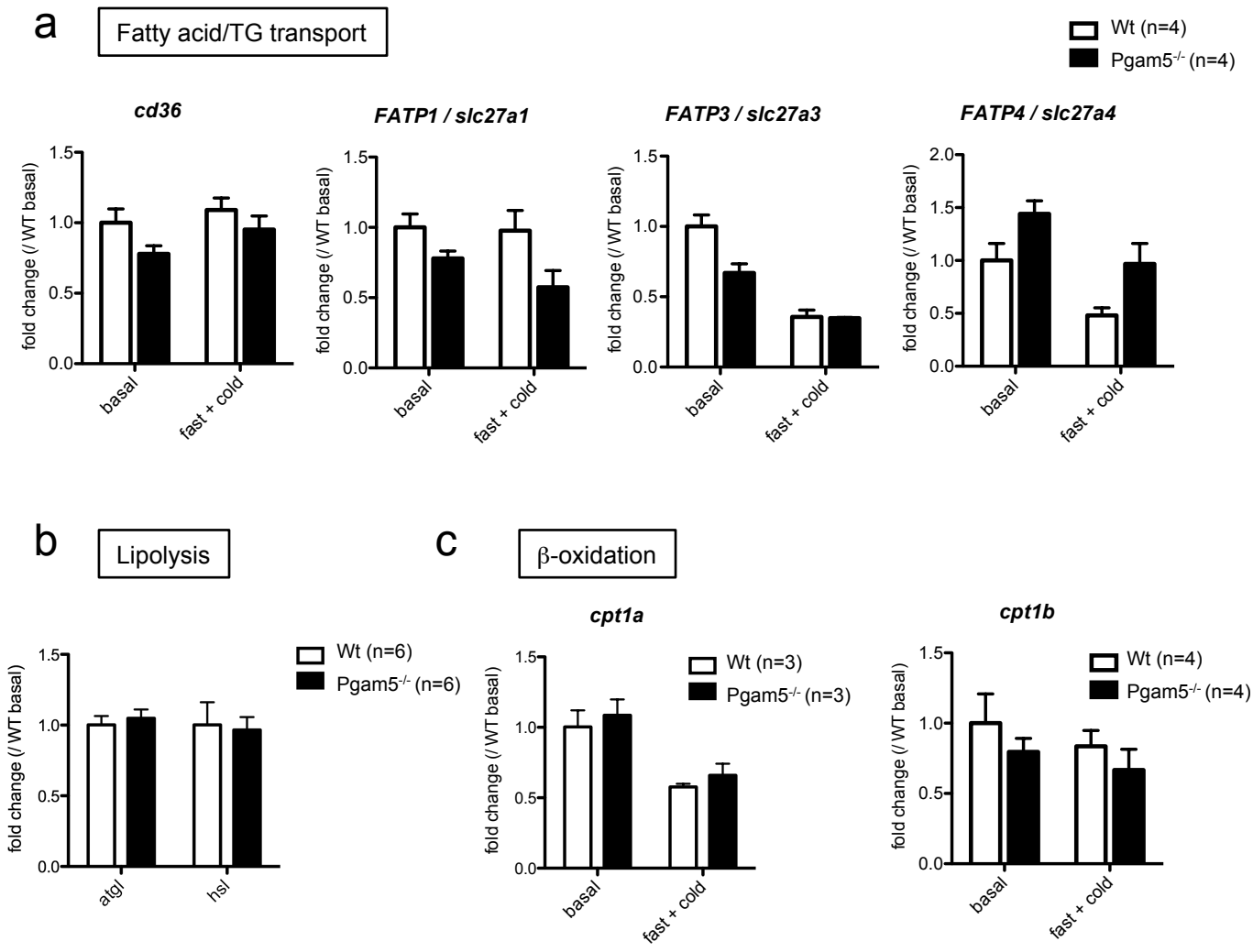

Supplementary Figure 3
Almost all the gene expression levels related to lipid metabolism in Pgam5-deficient BAT were comparable to those in Wt mice.

a

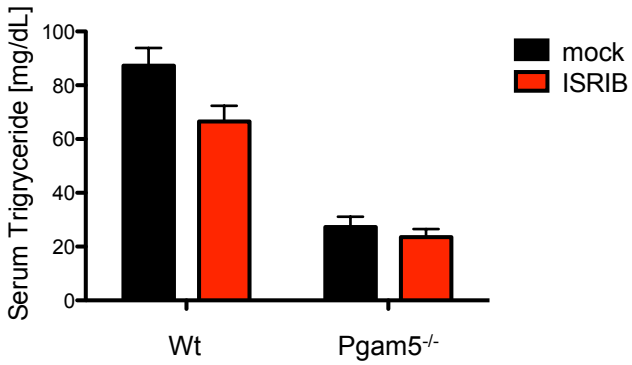

b

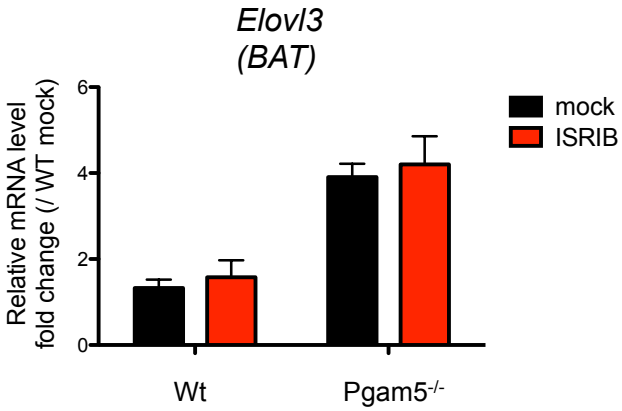

Supplementary Figure 4
The enhancement of lipid metabolism is not induced downstream of FGF21 induction.

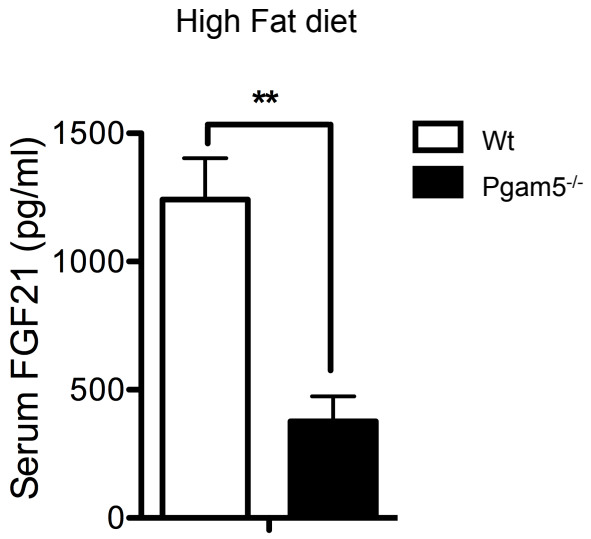

Supplementary Figure 5
Under high fat diet (HFD)-fed condition, serum FGF21 level is not enhanced in Pgam5 KO mice.

Supporting Information Figure legends

S1 Figure.

Generation of Pgam5 knockout (KO) mice.

(a) A schematic representation of the targeting vector and the targeting allele of the Pgam5 gene. The coding exons are depicted by orange boxes. Probes for Southern blot analysis are shown as blue and green lines. ScaI I, SpeI, restriction enzyme site; PGKp, phosphoglycerate kinase 1 promoter; neo, neomycin-resistant gene cassette; tk, thymidine kinase. (b) Genotyping of F1 mice (left panels) and homozygous mice (right panel). Genomic DNA extracted from mouse tails was examined by Southern blotting and PCR. The WT and mutant alleles were detected as 10.6- and 6.6-kb bands by the 5' probe and 16.6- and 10.6 kb bands by the 3' probe in Southern blotting and as 179- and 279-bp in PCR. (c) An immunoblot of PGAM5 in the primary cultured cells that were derived from WT and Pgam5 KO mice. MSF, mouse skin fibroblasts; MEF, mouse embryonic fibroblasts; BMDM, bone marrow-derived macrophages.

S2 Figure.

The expression levels of several genes related to adaptive thermogenesis in Pgam5

KO-mice-derived brown adipose tissue (BAT) are comparable to those in WT mice.

(a) Expression of the indicated genes in BAT from WT and Pgam5 KO mice under basal conditions or at 6 h of cold exposure after 12 h of fasting, as determined via quantitative RT-PCR (n=4). (b) Representative immunoblots for the indicated proteins derived from WT and Pgam5 KO mice under basal conditions or at 3 and 6 h of cold expose after 12 h of fasting. Data are expressed as the mean±SEM, **p<0.01, *p<0.05; two-way ANOVA/Bonferroni post-test (a).

S3 Figure.

Almost all the gene expression levels related to lipid metabolism in Pgam5-deficient BAT were comparable to those in WT mice.

(a, b, and c) Expression of the indicated genes related to lipid transporters (a), lipolysis (b), and β-oxidation (c) in BAT from WT and Pgam5 KO mice under basal conditions or at 6 h of cold exposure after 12 h of fasting, as determined via quantitative RT-PCR . Data are expressed as the mean±SEM (n=3-6).

S4 Figure.

The enhancement of lipid metabolism is not induced downstream of FGF21 induction.

(a and b) After fasting for 12 h, WT and Pgam5 KO mice were treated with 2.5 mg/kg body weight ISRIB or mock i.p. and subsequently exposed to cold stress. After 5 h, the triglyceride (TG) levels in the serum (a), and *Elovl3* gene expression in BAT (b), was determined. Data are expressed as the mean±SEM (WT; n=4 for each, Pgam5 KO; mock n=3, ISRIB n=4).

S5 Figure.

High-fat-diet (HFD)-fed conditions do not enhance serum FGF21 levels in Pgam5 KO mice.

The serum FGF21 concentration of WT and Pgam5 KO mice that were fed a HFD for 15 weeks was quantified by ELISA. Data are expressed as the mean±SEM (n=6 each), **$p<0.01$; unpaired Student's t-test**.**